



## UvA-DARE (Digital Academic Repository)

### Local orientational order in liquids revealed by resonant vibrational energy transfer

Panman, M.R.; Shaw, D.J.; Ensing, B.; Woutersen, S.

**DOI**

[10.1103/PhysRevLett.113.207801](https://doi.org/10.1103/PhysRevLett.113.207801)

**Publication date**

2014

**Document Version**

Final published version

**Published in**

Physical Review Letters

[Link to publication](#)

**Citation for published version (APA):**

Panman, M. R., Shaw, D. J., Ensing, B., & Woutersen, S. (2014). Local orientational order in liquids revealed by resonant vibrational energy transfer. *Physical Review Letters*, 113(20), 207801. <https://doi.org/10.1103/PhysRevLett.113.207801>

**General rights**

It is not permitted to download or to forward/distribute the text or part of it without the consent of the author(s) and/or copyright holder(s), other than for strictly personal, individual use, unless the work is under an open content license (like Creative Commons).

**Disclaimer/Complaints regulations**

If you believe that digital publication of certain material infringes any of your rights or (privacy) interests, please let the Library know, stating your reasons. In case of a legitimate complaint, the Library will make the material inaccessible and/or remove it from the website. Please Ask the Library: <https://uba.uva.nl/en/contact>, or a letter to: Library of the University of Amsterdam, Secretariat, Singel 425, 1012 WP Amsterdam, The Netherlands. You will be contacted as soon as possible.

*UvA-DARE is a service provided by the library of the University of Amsterdam (<https://dare.uva.nl>)*

## Local Orientational Order in Liquids Revealed by Resonant Vibrational Energy Transfer

M. R. Panman, D. J. Shaw, B. Ensing,<sup>\*</sup> and S. Woutersen<sup>†</sup>  
*Van 't Hoff Institute for Molecular Sciences (HIMS), University of Amsterdam,*  
*Science Park 904, 1098 XH Amsterdam, The Netherlands*

(Received 20 April 2014; revised manuscript received 25 June 2014; published 12 November 2014)

We demonstrate that local orientational ordering in a liquid can be observed in the decay of the vibrational anisotropy caused by resonant transfer of vibrational excitations between its constituent molecules. We show that the functional form of this decay is determined by the (distribution of) angles between the vibrating bonds of the molecules between which energy transfer occurs, and that the initial drop in the decay reflects the average angle between nearest neighbors. We use this effect to observe the difference in local orientational ordering in the two hydrogen-bonded liquids ethanol and *N*-methylacetamide.

DOI: 10.1103/PhysRevLett.113.207801

PACS numbers: 61.25.Em, 34.50.Ez, 64.70.Ja, 82.53.Eb

Many molecular liquids are believed to possess local structural ordering, in which neighboring molecules are preferentially at specific orientations with respect to each other. Such local orientational order in liquids is crucial for the properties of hydrogen-bonded liquids such as water [1], and evidence even exists that in these liquids phase transitions may occur in which the local orientational order is the order parameter [2–5]. As yet, local orientational order in liquids has been observed mostly in numerical simulations, and has been difficult to observe experimentally. Here, we show that local orientational order in liquids can be observed through its effect on the resonant transfer of vibrational excitations between the constituent molecules. Advances in ultrafast spectroscopy have made it possible to directly observe such intermolecular resonant vibrational energy transfer on surfaces [6], in clusters [7], in liquids [8–17], and in solids [18,19]. In these experiments, polarized optical excitation of a specific vibrational mode in part of the molecules creates an anisotropic distribution of excited transition-dipole moments, and resonant intermolecular transfer of the excitation causes this anisotropy to eventually vanish. We will show that the functional form of this anisotropy decay is determined mainly by the local orientational ordering of a liquid. We demonstrate this theoretically and experimentally, by comparing two hydrogen-bonded liquids with different local ordering.

In our calculation we assume that the energy transfer is incoherent (recent calculations on the OH-stretch resonant energy transfer in water suggest that this is a good approximation [20]) and caused by dipolar coupling, an approximation that has been validated by previous studies [6,7,14–16,18,19], and that the vibrational line shape is homogeneous on the time scale of the energy transfer. Nondipolar effects [21], coherence [22], and spectral inhomogeneity [11–13] can all be incorporated in a straightforward manner to obtain more accurate results, but these effects do not influence our main conclusions. For

two vibrational modes  $i$  and  $j$  with transition-dipole moments  $\boldsymbol{\mu}_i$  and  $\boldsymbol{\mu}_j$  located at  $\mathbf{r}_i$  and  $\mathbf{r}_j$ , the dipolar coupling is [23]

$$V_{ij} = \frac{\mu_i \mu_j}{4\pi\epsilon_0 r_{ij}^3} [\mathbf{e}_{\mu_i} \cdot \mathbf{e}_{\mu_j} - 3(\mathbf{e}_{r_{ij}} \cdot \mathbf{e}_{\mu_i})(\mathbf{e}_{\mu_j} \cdot \mathbf{e}_{r_{ij}})], \quad (1)$$

where  $\mu_i = |\boldsymbol{\mu}_i|$  and  $r_{ij} = |\mathbf{r}_i - \mathbf{r}_j|$ , and where  $\mathbf{e}_{\mu_i} = \boldsymbol{\mu}_i/\mu_i$  and  $\mathbf{e}_{r_{ij}} = (\mathbf{r}_i - \mathbf{r}_j)/r_{ij}$  are unit vectors, so that the term in square brackets (generally referred to as the orientation factor) depends only on the relative orientation of the two transition-dipole moments. The rate of energy transfer is given by Fermi's golden rule [24]:

$$k_{ij} = \frac{2\pi}{\hbar} |V_{ij}|^2 \int \sigma_i(E) \sigma_j(E) dE, \quad (2)$$

where  $\sigma_{i,j}(E)$  are the normalized line shapes of the vibrational modes between which transfer occurs. In a liquid, energy transfer between each possible pair of transition-dipole moments  $i$  and  $j$  can occur, and the probability  $p_i$  of a vibrational excitation being located on the  $i$ th molecule will in general be time dependent.

In a vibrational pump-probe experiment, a small fraction of the molecules in a liquid is excited from the  $v = 0$  to the  $v = 1$  state of a specific intramolecular (typically stretching) mode using a linearly polarized resonant infrared pulse. The probability for a vibrational excitation to be at molecule  $i$  is then proportional to  $\cos^2 \theta_i$ , where  $\theta_i$  is the angle between the transition-dipole moment of the molecule and the polarization of the excitation pulse (here defined to be in the  $z$  direction). Resonant transfer of the excitation between the molecules causes this anisotropic excitation-probability distribution to eventually become isotropic, so that the anisotropy, defined as  $R = \langle \frac{1}{2}(3\cos^2\theta - 1) \rangle$  (with  $\theta$  the angle between the transition dipole of the excited molecules and the excitation

polarization, and  $\langle \dots \rangle$  denoting ensemble averaging), decays from  $\frac{2}{3}$ , the value for the initial  $\cos^2 \theta$  distribution, to zero, the value for an isotropic distribution. The functional form of the decay of  $R$  is determined by the time evolution of the excitation-probability distribution. From the conformation of the liquid, the complete set of transfer rates  $k_{ij}$  can be calculated using Eqs. (1) and (2), and the master equation for the time-dependent excitation probabilities is [20]

$$\frac{dp_i}{dt} = \sum_{j \neq i} k_{ij} p_j - p_i \sum_{j \neq i} k_{ij}, \quad (3)$$

where  $p_i$  is the probability of molecule  $i$  being in the  $v = 1$  state. The excitation-probability distribution at  $t = 0$  is given by  $p_i(0) \propto \cos^2 \theta_i$  (where  $\theta_i$  is the angle of transition-dipole moment  $i$  with the excitation polarization), and the anisotropy at any subsequent time  $t$  is given by

$$\begin{aligned} R(t) &= \left\langle \frac{1}{2} (3 \cos^2 \theta - 1) \right\rangle \\ &= \sum_i \frac{1}{2} (3 \cos^2 \theta_i - 1) p_i(t) / \sum_i p_i(t). \end{aligned} \quad (4)$$

It should be noted that the random motion of the molecules also contributes to the decay of  $R$ . This additional contribution can be included in the theoretical description [14], but for the liquids and time scales investigated here, it can be neglected (see below).

From Eqs. (1)–(4) we can see that the functional form of the anisotropy decay  $R(t)$  is remarkably insensitive to some of the properties of a liquid. In particular, from Eqs. (3) and (4) it can be seen directly that scaling all the  $k_{ij}$  by the same factor  $s$  will change the time dependences of the excitation probabilities from  $p_i(t)$  to  $p_i(st)$ , and so leads to an anisotropy decay  $R(st)$ ; that is, it will renormalize the time dependence by a factor  $s$ , without any change in the functional form of the anisotropy decay. An example would be expanding or compressing the liquid (without changing the angles between the molecules). Such a volume change by a factor  $a$  corresponds to multiplying all distances  $r_{ij}$  by a factor  $a^{1/3}$ , and therefore scaling all rates  $k_{ij}$  by a factor  $a^{-2}$  [see Eqs. (1) and (2)], so its only effect is to replace  $R(t)$  by  $R(a^{-2}t)$ , a time renormalization. Largely the same holds for the spectral properties, represented by the integral in Eq. (2). If the line shape function  $\sigma(E)$  of the liquid changes (for instance due to a change in temperature), then the integral in Eq. (2) changes value, but since this causes all the  $k_{ij}$  to change by the same factor, the result is again a renormalization of the time dependence of  $R(t)$ , but no change in the functional form.

The main determinant of the functional form of  $R(t)$  is in fact the orientation factor in Eq. (1). This will be demonstrated below by explicit calculations and experiments, but

it can already be understood from simple qualitative argumentation (see Fig. 1). Because of the very strong ( $r^{-6}$ ) distance dependence of the transfer rate, the transfer to nearby molecules occurs much faster than that to more distant molecules. The orientation dependence of the rate will scramble this relation between distance and transfer rate, but only to a small extent [25]. The relation between distance and rate has direct consequences for the functional form of the anisotropy decay: at short times, the decay is determined by transfer to nearby molecules, at long times by transfer to more distant ones. In particular, the initial drop at the shortest times is determined mainly by energy transfer to the nearest neighbors of the initially excited molecule. The magnitude of this initial drop therefore depends strongly on the angle between nearest-neighbor transition dipoles. It can be shown [26] that if the angle between the donor and acceptor is  $\delta$ , then transfer of the vibrational excitation causes the anisotropy to decrease from  $\frac{2}{3}$  to  $\frac{1}{3}(3 \cos^2 \delta - 1)$ . Hence, the larger the angle  $\delta$  between the transition dipole moments of the nearest neighbors, the larger is the initial decrease in the anisotropy: the initial drop in anisotropy at short times, which is determined mostly by energy transfer to nearest neighbors, is much larger if neighboring transition-dipole moments in a liquid are at a nonzero angle than when they are approximately parallel, see Fig. 1 for a schematic illustration. The anisotropy decay at longer times is mostly caused by transfer to molecules that are further away, and since for large enough distances there is no correlation between molecular orientations, for sufficiently long delay times the anisotropy decay becomes similar for all liquids.

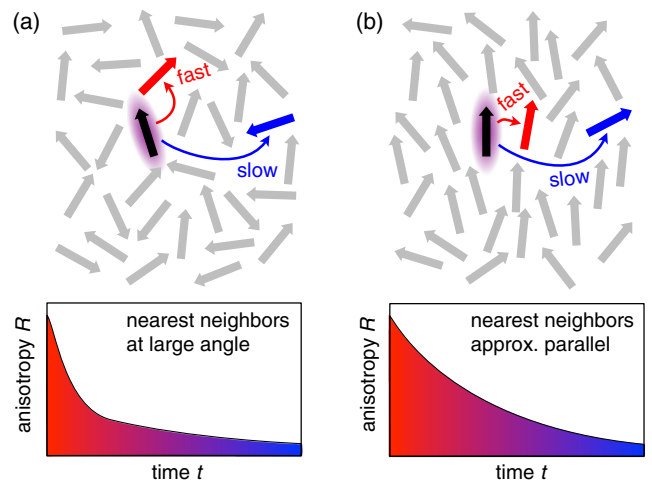


FIG. 1 (color online). Schematic representation of how the structure of a liquid influences the functional form of the vibrational anisotropy decay. Each arrow represents the vibrational transition-dipole moment of a molecule. The initial drop in the vibrational anisotropy is larger for a liquid in which nearest neighbors are at a large angle (a) than for a liquid in which they are approximately parallel (b).

To quantitatively investigate the relation between liquid structure and anisotropy decay, we performed molecular dynamics (MD) simulations of two hydrogen-bonded liquids for which evidence exists that the angles between nearest neighbors are very different: ethanol ( $\text{CH}_3\text{-CH}_2\text{-OH}$ , EtOH) and liquid *N*-methylacetamide ( $\text{CH}_3\text{-NH-CO-CH}_3$ , NMA). Simulations and experiments have shown evidence that in NMA the molecules form linear chains connected by  $\text{NH}\cdots\text{OC}$  hydrogen bonds, such that neighboring NH groups are approximately parallel [27–29], whereas in ethanol hydrogen bonding occurs between the OH group of one molecule and a lone-electron pair on the O atom of another, such that the angle between two hydrogen-bonded OH groups is approximately  $180^\circ - 109.5^\circ \approx 70^\circ$  [30,31]. This difference in local ordering is also observed in our MD simulations [32]. Figure 2 shows the distribution of the angles between neighboring OH groups in ethanol, and of the angles between neighboring NH groups in NMA (where OH or NH groups are considered neighbors if their distance is less than the first minimum in their radial distribution function). In ethanol, hydrogen-bonded neighbors clearly tend to be at a nonzero angle with respect to each other, whereas in NMA they tend to be more aligned. In both liquids, there is a uniform, angle-independent background due to the non-hydrogen-bonded neighbors.

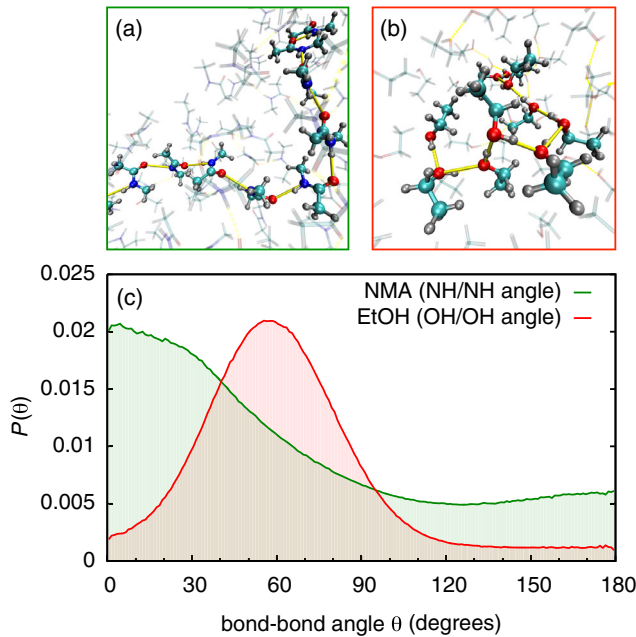


FIG. 2 (color online). (a),(b) Snapshots of the MD simulations of liquid NMA (a) and ethanol (b). (c) Distribution of the angle between nearest-neighbor NH bonds in NMA, and the same for OH bonds in ethanol. Two bonds are defined to be nearest neighbors if their distance is less than the minimum in their radial distribution function. The positions of the maxima show that neighboring NH bonds in NMA are approximately parallel, whereas neighboring OH bonds in ethanol are mostly at a nonzero angle.

To derive the anisotropy decay due to energy transfer from the MD simulations we proceed as follows. We assume that energy transfer occurs much faster than the orientational random motion of the OH and NH bonds, which also causes the anisotropy to decay. For EtOH and NMA the rotational correlation times are 18 [35] and  $>30$  ps [36], so for the experimentally investigated time range ( $\leq 3$  ps) this assumption is certainly valid. By integrating Eq. (3) and using Eq. (4) we calculate the anisotropy decay [32]. The result is shown in Fig. 3 as the solid curves. In this graph we plot  $R$  as a function of reduced (dimensionless) time

$$\tau = \left[ \frac{2\pi}{\hbar} \left( \frac{\mu^2}{4\pi\epsilon_0 a_0^3} \right)^2 \int \sigma(E)^2 dE \right] t,$$

where  $a_0 = n^{-1/3}$  with  $n$  the number density. The functional form of  $R(\tau)$  obtained in this way is independent of density,

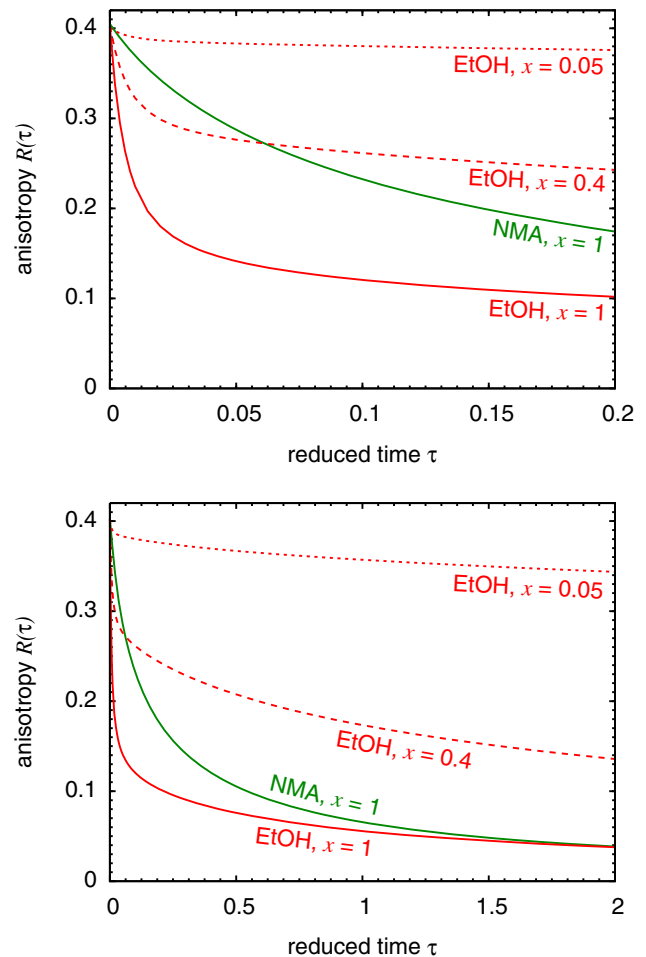


FIG. 3 (color online). Calculated vibrational anisotropy decay for NMA and ethanol at different isotopic dilutions  $x$  ( $x=1$  is the isotopically pure liquid), for different ranges of the reduced time  $\tau$ . Note that for long  $\tau$  the curves approach the same asymptotic behavior since for long intermolecular distance there is no correlation between the orientation of the donor and acceptor molecules.



transition-dipole-moment magnitude, and spectral density (see the discussion above). In both liquids, the anisotropy at  $t = 0$  is  $\frac{2}{3}$ , but clearly the initial decrease in  $R(\tau)$  is much larger in ethanol than in NMA. Plotting the data with a logarithmic time axis shows that the difference between NMA and ethanol is not simply due to a difference in the magnitude of their transition-dipole moments [32]. That this difference is rather a consequence of the different distributions of nearest-neighbor angles in the two liquids can be seen by comparing the anisotropy decay for isotopically diluted EtOH. In Fig. 3 we show the result for isotopic fractions of  $x = 0.4$  and  $x = 0.05$ . Clearly, the more dilute the EtOH/EtOD mixture, the less is the initial drop in  $R$ . This is because in the isotopically diluted liquid an excited transition dipole will no longer have a resonant nearest neighbor, so the energy transfer still occurs, but more slowly (because of the larger distance), and to transition dipoles that are at arbitrary angles to the initially excited one. Note that for long times ( $\tau > 1$ ), the decays of NMA and EtOH eventually become similar, since the decay at these delays is caused by transfer from initially excited OH (NH) groups to more distant OH (NH) groups, so that no orientational correlation between acceptor and donor exists, and the decay converges to that of a completely structureless liquid.

The calculations on NMA and ethanol show that differences in local orientational ordering result in different anisotropy decays. This functional relation between the orientational order and anisotropy decay is not invertible, and so the most accurate way of deriving information from the anisotropy decay would be to predict  $R(t)$  from different proposed liquid structures and compare to the experimentally observed  $R(t)$ . But even without such modeling, it is already possible to derive some information about the angular distribution from the observed  $R(t)$ . The magnitude of the initial drop in the anisotropy increases with increasing angle between nearest-neighbor liquid molecules. This explains the difference between NMA (no initial drop, as the nearest neighbors are approximately parallel) and ethanol (large initial drop, nearest neighbors at  $\approx 60^\circ$ ). This qualitative relation can even be made semiquantitative. If an excitation is transferred to a transition dipole that is at an angle  $\theta$  with respect to the initially excited one, the anisotropy drops by a factor  $P_2(\cos \theta)$ , where  $P_2(x) = \frac{1}{2}(3x^2 - 1)$  is the second Legendre polynomial [26]. Hence, if the nearest-neighbor angular dipole-dipole distribution peaks at  $\theta_{\max}$ , and a molecular transition dipole has  $n$  neighbors, then the factor by which the anisotropy drops initially can be approximated by  $(1/n) + ((n-1)/n)P_2(\cos \theta_{\max})$ . For ethanol, we have  $n = 2$  [it forms hydrogen-bonded chains [30,31], and  $\theta_{\max} \approx 60^\circ$ , see Fig. 2(c)], so we obtain a factor of  $\frac{1}{4}$ , in reasonable agreement with the experimentally observed drop from 0.4 to  $\approx 0.1$  observed in the simulation and in the experiment (Figs. 3 and 4). Conversely, if the number of nearest neighbors is known, the initial drop in anisotropy can

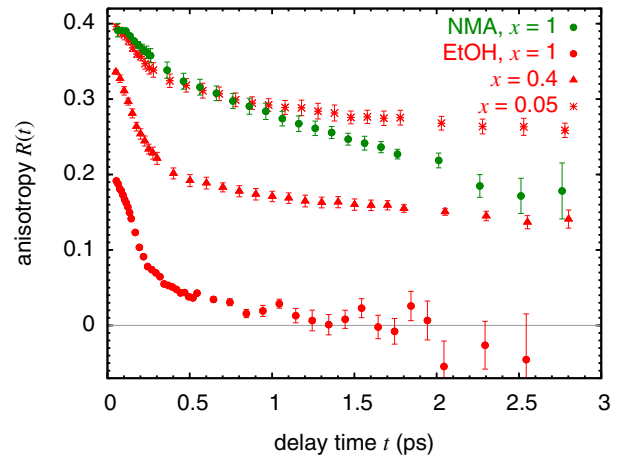


FIG. 4 (color online). Experimentally observed vibrational anisotropy decay for NMA and ethanol at different isotopic dilutions  $x$  ( $x = 1$  is the isotopically pure liquid).

in principle be used to obtain a rough estimate of the nearest-neighbor angle. In the case of a probability distribution  $p(\theta)$  of nearest-neighbor angles, the initial drop in  $R(t)$  is  $1/n + ((n-1)/n)\langle P_2(\cos \theta) \rangle$ , where  $\langle \dots \rangle$  denotes the average over the distribution  $p(\theta)$ .

To investigate if the predicted differences in the local liquid structures of NMA and ethanol can be observed experimentally, we measure the decay of the anisotropy of the NH- and OH-stretch modes of these two liquids [32]. The results are shown in Fig. 4. We find that the predicted difference in the functional form of  $R(\tau)$  is indeed clearly observable. In particular, in EtOH a pronounced initial drop of  $R(t)$  is observed, which is absent in NMA (the NMA and ethanol data cannot be overlapped by rescaling the time axis [32]). We also observe that in isotopic EtOH/EtOD mixtures, this initial drop decreases in magnitude with increasing dilution, as predicted (see Fig. 3). The agreement between theory and experiment is not perfect: the predicted very sharp initial decrease in ethanol is probably too fast for our temporal resolution (and causes the initial value to be  $< 0.4$  due to convolution), and for long times the experimentally observed anisotropy in EtOH decays faster than theoretically predicted. This might be because the simulations overestimate the local ordering in liquid EtOH, or because of orientational random motion, which was not included in the present theoretical analysis, and part of which occurs on a picosecond time scale [37,38].

To conclude, our results show that the functional form of the vibrational-anisotropy decay is determined by the local orientational ordering of the molecules in a liquid. As a probe of liquid orientational correlation, this effect may serve as a complement to (*x*-ray or neutron) scattering experiments which provide access to distance correlation in liquids, although the mathematical relation between observation and molecular correlation is not as straightforward in the former as it is in the latter. Interestingly, by measuring

the decay of the anisotropy for different vibrational modes in the molecules of a liquid, it can even be determined which particular parts of these molecules are locally ordered, and if so, at which (average) angle. Finally, as already mentioned, a more detailed theoretical analysis should include effects such as random orientational motion, spectral inhomogeneity, coherence, and nondipolar contributions to the intermolecular coupling. We hope that the results presented here will stimulate work in this direction.

The authors kindly acknowledge Huib Bakker for valuable discussions. This work is part of the research programme of the Foundation for Fundamental Research on Matter (FOM), which is part of the Netherlands Organisation for Scientific Research (NWO).

\*Corresponding author.

b.ensing@uva.nl

†Corresponding author.

s.woutersen@uva.nl

- [1] J. R. Errington and P. D. Debenedetti, *Nature (London)* **409**, 318 (2001).
- [2] R. Kurita and H. Tanaka, *Science* **306**, 845 (2004).
- [3] L. Liu, S.-H. Chen, A. Faraone, C.-W. Yen, and C.-Y. Mou, *Phys. Rev. Lett.* **95**, 117802 (2005).
- [4] H. Tanaka, *Eur. Phys. J. E* **35**, 113 (2012).
- [5] K. Murata and H. Tanaka, *Nat. Commun.* **4**, 2844 (2013).
- [6] M. Bonn, C. Hess, and M. Wolf, *J. Chem. Phys.* **115**, 7725 (2001).
- [7] K. J. Gaffney, I. R. Piletic, and M. D. Fayer, *J. Chem. Phys.* **118**, 2270 (2003).
- [8] M. L. Cowan, B. D. Bruner, N. Huse, J. R. Dwyer, B. Chugh, E. T. J. Nibbering, T. Elsaesser, and R. J. D. Miller, *Nature (London)* **434**, 199 (2005).
- [9] J. Lindner, P. Vohringer, M. S. Pshenichnikov, D. Cringus, D. A. Wiersma, and M. Mostovoy, *Chem. Phys. Lett.* **421**, 329 (2006).
- [10] D. Kraemer, M. L. Cowan, A. Paarmann, N. Huse, E. T. J. Nibbering, T. Elsaesser, and R. J. D. Miller, *Proc. Natl. Acad. Sci. U.S.A.* **105**, 437 (2008).
- [11] A. Paarmann, T. Hayashi, S. Mukamel, and R. J. D. Miller, *J. Chem. Phys.* **130**, 204110 (2009).
- [12] M. Yang and J. L. Skinner, *Phys. Chem. Chem. Phys.* **12**, 982 (2010).
- [13] T. L. Jansen, B. M. Auer, M. Yang, and J. L. Skinner, *J. Chem. Phys.* **132**, 224503 (2010).
- [14] M. Yang, F. Li, and J. L. Skinner, *J. Chem. Phys.* **135**, 164505 (2011).
- [15] A. A. Bakulin, D. Cringus, P. A. Pieniazek, J. L. Skinner, T. L. C. Jansen, and M. S. Pshenichnikov, *J. Phys. Chem. B* **117**, 15545 (2013).
- [16] S. M. Gruenbaum and J. L. Skinner, *J. Phys. Chem.* **139**, 175103 (2013).
- [17] K. Ramasesha, L. D. Marco, A. Mandal, and A. Tokmakoff, *Nat. Chem.* **5**, 935 (2013).
- [18] R. L. A. Timmer and H. J. Bakker, *J. Phys. Chem. A* **114**, 4148 (2010).
- [19] H. Chen, X. Wen, J. Li, and J. Zheng, *J. Phys. Chem. A* **118**, 2463 (2014).
- [20] M. Yang, *Bull. Korean Chem. Soc.* **33**, 885 (2012).
- [21] H. Torii, *J. Phys. Chem. B* **114**, 13403 (2010).
- [22] H. Torii, *J. Phys. Chem. A* **110**, 9469 (2006).
- [23] J. D. Jackson, *Classical Electrodynamics* (Wiley, New York, 1999).
- [24] B. Henderson and G. F. Imbusch, *Optical Spectroscopy of Inorganic Solids* (Oxford University Press, Oxford, 1989).
- [25] To understand this, consider as an example the case of two parallel transition dipole moments, for which the orientation factor is  $1 - 3 \cos^2 \phi$ , with  $\phi$  the angle between the direction of the dipole moments and the distance vector connecting them. This orientation factor has a maximum value of 1, and vanishes when  $\phi = 54.7^\circ$ . Doubling the distance decreases the energy-transfer rate by a factor of 64. To achieve the same reduction in rate by changing the relative orientation of the two transition dipoles, the orientation angle  $\phi$  must be within  $2.6^\circ$  of  $54.7^\circ$ ; even librational motion is sufficient to prevent this from happening. Hence, the relation between distance and energy-transfer rate is only slightly blurred by the orientational dependence of the transfer rate.
- [26] A. Szabo, *J. Chem. Phys.* **81**, 150 (1984).
- [27] H. Torii and M. Tasumi, *J. Raman Spectrosc.* **29**, 81 (1998).
- [28] T. W. Whitfield, G. J. Martyna, S. Allison, S. P. Bates, H. Vass, and J. Crain, *J. Phys. Chem. B* **110**, 3624 (2006).
- [29] D. A. Turton and K. Wynne, *J. Chem. Phys.* **128**, 154516 (2008).
- [30] C. J. Benmore and Y. L. Loh, *J. Chem. Phys.* **112**, 5877 (2000).
- [31] A. Vrhovšek, O. Gereben, A. Jamnik, and L. Pusztai, *J. Phys. Chem. B* **115**, 13473 (2011).
- [32] See Supplemental Material at <http://link.aps.org/supplemental/10.1103/PhysRevLett.113.207801>, which includes Refs. [33,34], for the details of the MD simulation and the pump-probe experiments, and for a logarithmic plot of the data.
- [33] P. Hamm, R. A. Kaindl, and J. Stenger, *Opt. Lett.* **25**, 1798 (2000).
- [34] Y. L. A. Rezus and H. J. Bakker, *J. Phys. Chem. A* **112**, 2355 (2008).
- [35] T. D. Ferris and T. C. Farrar, *Mol. Phys.* **100**, 303 (2002).
- [36] C. G. Seipelt and M. D. Zeidler, *Ber. Bunsen-Ges. Phys. Chem.* **101**, 1501 (1997).
- [37] J. Barthel, K. Bachhuber, R. Buchner, and H. Hetzenauer, *Chem. Phys. Lett.* **165**, 369 (1990).
- [38] J. T. Kindt and C. A. Schmittenmaer, *J. Phys. Chem.* **100**, 10373 (1996).